

A neural network-based frequency and severity model for insurance claims

Dong-Young Lim

Department of Industrial Engineering
Ulsan National Institute of Science and Technology (UNIST)
South Korea

February 27, 2024

Abstract

This paper proposes a flexible and analytically tractable class of frequency and severity models for predicting insurance claims. The proposed model is able to capture nonlinear relationships in explanatory variables by characterizing the logarithmic mean functions of frequency and severity distributions as neural networks. Moreover, a potential dependence between the claim frequency and severity can be incorporated. In particular, the paper provides analytic formulas for mean and variance of the total claim cost, making our model ideal for many applications such as pricing insurance contracts and the pure premium. A simulation study demonstrates that our method successfully recovers nonlinear features of explanatory variables as well as the dependency between frequency and severity. Then, this paper uses a French auto insurance claim dataset to illustrate that the proposed model is superior to the existing methods in fitting and predicting the claim frequency, severity, and the total claim loss. Numerical results indicate that the proposed model helps in maintaining the competitiveness of an insurer by accurately predicting insurance claims and avoiding adverse selection.

KEYWORDS: frequency-severity model; dependence modeling; aggregate risk loss; neural network-based model

1 Introduction

We are interested in estimating the total claim cost incurred by an insurer when characteristics of a policyholder such as age, driving history, insurance history and so on are given. This task is

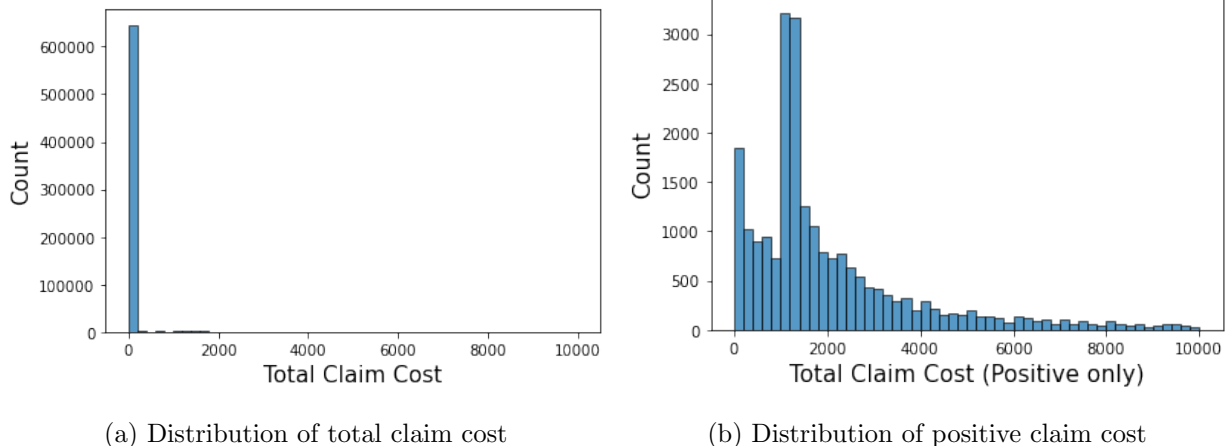


Figure 1: Histograms of total claim cost in the auto insurance claims data. The left figure shows the histogram of total claim cost and the right figure shows the histogram of positive total claim cost.

particularly important in insurance business as it is directly linked to computing the pure premium and classifying risk groups in a portfolio of policies. However, the estimation of the total claim cost is not straightforward because the target distribution is typically zero-inflated and right-skewed. For example, Figure 1 shows the histogram of the total claim loss from a French auto insurance dataset, in which most samples record zero claims and the size of claim loss can be extremely high. Usual predictive models based on supervised learning or regressions with the normality assumption may not be suitable for dealing with such type of data.

More specifically, we consider a random variable Z to be defined by

$$Z = \begin{cases} \sum_{k=1}^N Y_k & \text{if } N > 0, \\ 0 & \text{if } N = 0, \end{cases} \quad (1)$$

where N is a nonnegative integer-valued random variable and $\{Y_k\}_{k \in \mathbb{N}}$ is a sequence of independent and identically distributed random variables. In the context of insurance claims, the random variables N , Y_k and Z represent the number of claims (frequency), the amount of the k -th claim (severity), and the total claim cost, over a fixed time period for a policyholder, respectively. The traditional generalized linear model (GLM) with a log link function assumes that N is independent of $\{Y_k\}_{k \in \mathbb{N}}$, and then specifies the logarithmic mean functions of N and Y_k as linear functions of a vector of explanatory variables $\mathbf{x} \in \mathbb{R}^p$:

$$\log \mathbb{E}[N|\mathbf{x}] = \alpha^\top \mathbf{x} \quad \text{and} \quad \log \mathbb{E}[Y_k|\mathbf{x}] = \beta^\top \mathbf{x}, \quad (2)$$

where $\alpha \in \mathbb{R}^p$ and $\beta \in \mathbb{R}^p$ are the regression coefficients for the frequency and severity models. In such a setting, the expected total claim cost of \mathbf{x} is simply computed by, due to the independence

assumption between N and $\{Y_k\}_{k \in \mathbb{N}}$,

$$\mathbb{E}[Z|\mathbf{x}] = \mathbb{E}[N|\mathbf{x}]\mathbb{E}[Y_1|\mathbf{x}] = \exp\{(\alpha^\top + \beta^\top)\mathbf{x}\}.$$

However, it is well recognized that the traditional GLM has two major drawbacks when applied in practice. On one hand, the number of claims N and the amount of claims $\{Y_k\}_{k \in \mathbb{N}}$ are assumed to be independent. The model without taking account of a dependence effect between frequency and severity is inevitably faced with model risk and yields an inaccurate result in estimating the total claim cost when there exists a statistical association between frequency and severity. Indeed, it is known that the amount of the average severity is negatively related to the number of claims in auto insurance claims data, see [Shi et al. \[2015\]](#) and [Garrido et al. \[2016\]](#). On the other hand, the structure of the logarithmic mean functions of N and Y is restricted to a linear form as in (2), which is too rigid to capture complex nonlinear relationships from explanatory variables. For example, the nonlinearity in explanatory variables and its effects on frequency-severity models have been investigated in [Kelly and Nielson \[2006\]](#), [Guelman \[2012\]](#) and [Yang et al. \[2018\]](#).

Several papers attempted to overcome the limitation of the traditional GLM by incorporating the dependence between frequency and severity within the GLM framework. In [Gschlößl and Czado \[2007\]](#), [Frees et al. \[2011a\]](#) and [Garrido et al. \[2016\]](#), the frequency variable is utilized as an explanatory variable for the severity distribution to allow for a linear dependence between frequency and severity. [Czado et al. \[2012\]](#) and [Kramer et al. \[2013\]](#) extended the traditional GLM by combining the marginal frequency and severity distributions through a bivariate copula. The aforementioned ideas were extensively reviewed and compared in [Shi et al. \[2015\]](#). Despite such developments in the literature, the GLM based methods have their obvious shortcoming on capturing the nonlinearity in the data, and often require additional effort to resolve multicollinearity in regression models.

Another important stream of the literature on frequency-severity models is to use modern machine learning techniques for predicting insurance claims. Along with a significant increase in available data and computing power, machine learning approaches provide an excellent vehicle for fully extracting a complex relationship in the dataset. For example, [Yang et al. \[2018\]](#) introduced a gradient boosting algorithm to the nonlinear Tweedie compound Poisson model for predicting insurance premium and [Zhou et al. \[2020\]](#) extended it to the zero-inflated Tweedie model. [Huang and Meng \[2019\]](#) investigated several machine learning techniques to predict the risk probability and claim frequency of an insured vehicle using telematics driving data. However, these models directly or implicitly assume that frequency and severity are independent. While [Guelman \[2012\]](#) and [Su and Bai \[2020\]](#) considered the dependency between frequency and severity by separately applying gradient boosting to frequency and severity distributions, it is not possible to compute the *exact* mean and variance of the total claim cost under their models.

In this paper, we focus on modeling frequency and severity distributions to estimate the total claim cost based on neural networks. We call this novel framework *the neural frequency and severity (NeurFS) model*. In particular, we unify advantages of the existing models from different fields, namely machine learning and actuarial science, to build a novel class of frequency and severity models that captures the nonlinearity and the dependence in the insurance claims dataset. Specifically, the transformed mean functions of frequency and severity distributions are characterized by neural networks. The use of neural networks allows our model to automatically extract complex relations in data, and to efficiently handle large-scale data. Furthermore, the proposed model introduces the possible dependence between frequency and severity components by considering the frequency variable as an additional explanatory variable for the average severity. A simulation study based on a synthetic dataset demonstrates that the proposed model accurately fits and predicts the frequency and severity components, and the total claim amount. As a real-world application, we apply our model to the French auto insurance claim data and find that the proposed model outperforms the existing models in terms of various evaluation metrics.

The proposed model has several strengths over the existing methods. Firstly, the paper provides the explicit closed-form solutions for mean and variance of the total claim cost in the presence of the non-linearity and dependence structure in insurance claims data. Secondly, a wide range of probability distributions can be utilized for marginal frequency and severity distributions in our modeling framework. In this paper, we mainly consider the exponential family of distributions due to its popularity. Thirdly, we suggest efficient neural network architectures to estimate parameters of the model. In our training scheme, the parameters of neural networks and distribution parameters are simultaneously estimated by solving the associated optimization problems. Lastly, compared to directly modeling the total claim cost Z without decomposing it into frequency and severity components, our approach aligns with common risk analysis methods used by insurance companies, which consider the likelihood of an event occurring and the potential magnitude of each event separately. This separation facilitates more targeted risk management strategies.

Building on these strengths, it is important to highlight the broader applicability of our approach. The proposed model can be applied to a wide range of data types, represented as a random sum defined in (1). This includes classification of territory risk, operational risk modeling and health care expenditure prediction [Dahen and Dionne, 2010, Brechmann et al., 2014, Urbina and Guillén, 2014, Frees et al., 2011a, Xie and Gan, 2023]. We also refer to Radanliev and Roure [2023] for an insightful overview of new and emerging forms of data.

This paper is organized as follows. In Section 2, we develop the NeurFS model with some assumptions. In Section 3, we present some background on neural networks and notations. Also, we describe the estimation process and the network architecture. Section 4 demonstrates the accuracy

and effectiveness of our model through an artificial example. In Section 5, we apply the NeurFS model to real insurance claims data and compare the performance of the proposed model with that of the existing models in the literature.

2 Neural Frequency-Severity Model

Section 2.1 introduces two marginal distributions for frequency-severity models and assumptions required to obtain main results, while Section 2.2 presents the NeurFS model and provides analytic formulas for the mean and variance of the total claim cost.

2.1 Marginal Distributions and Assumptions

Recall that a nonnegative integer-valued random variable N represents frequency for a fixed time period. We also use the term, the number of claims, to represent the random variable N . We assume that there exists some constant $\delta > 0$ such that, for $t \in \mathcal{I}_N := (-\delta, \delta)$, the moment generating function of N is finite:

$$M_N(t) := E[e^{tN}] < \infty.$$

That is, $M_N(t)$ is well-defined within the interval \mathcal{I}_N . We then have the following useful identity for the k -th order derivative of $M_N(t)$ evaluated at $t = \gamma$:

$$M_N^{(k)}(\gamma) := \left. \frac{\partial^k M_N(t)}{\partial t^k} \right|_{t=\gamma} = E[N^k e^{\gamma N}] \quad (3)$$

for $\gamma \in \mathcal{I}_N$. A common and popular choice for N is the Poisson distribution. In the case of the Poisson distribution, $M_N(t)$ is finite for all $t \in \mathbb{R}$, i.e., $\mathcal{I}_N = (-\infty, \infty)$. Moreover, several parametric counting distributions have been discussed to accommodate the excess zero observations and over-dispersion observed in fitting claim frequency data. Our framework can adopt these distributions in modeling the frequency distribution. We list popular counting distributions, and information on their moment generating functions in Table 1 and Table 3.

From the definition of the total claim cost in (1), one can define the average claim severity by

$$\bar{Y} := \frac{Z}{N} = \begin{cases} \frac{1}{N} \sum_{k=1}^N Y_k & \text{if } N > 0, \\ 0 & \text{if } N = 0, \end{cases} \quad (4)$$

and then we have $Z = N\bar{Y}$. Here, we assume that $\{Y_k\}_{k=1}^N$ are mutually independent and identically distributed random variables conditioned by N and that the mean of the average severity depends on N . Moreover, we assume that the individual claim severity distribution belongs to the exponential

Frequency distributions			
Models	pmf	$E[N]$	$Var[N]$
Binomial(λ, m)	$\binom{m}{n} \left(\frac{\lambda}{m}\right)^n \left(1 - \frac{\lambda}{m}\right)^{m-n}$	λ	$\lambda \left(1 - \frac{\lambda}{m}\right)$
Poisson(λ)	$\frac{e^{-\lambda} \lambda^n}{n!}$	λ	λ
ZIP(λ, π)	$\pi + (1 - \pi)e^{-\lambda}, \quad n = 0$ $(1 - \pi) \frac{e^{-\lambda} \lambda^n}{n!}, \quad n = 1, 2, \dots$	$(1 - \pi)\lambda$	$(1 - \pi)(\lambda + \pi\lambda^2)$
NB(π, r)	$\frac{\Gamma(n+r)}{n!\Gamma(r)} \pi^r (1 - \pi)^n, \quad n = 0, 1, \dots$	$\frac{r(1-\pi)}{\pi}$	$\mu \left(1 + \frac{\mu}{r}\right)$

Table 1: A summary of frequency distributions

dispersion family (EDF) because several distributions commonly used for modeling severity such as gamma distribution, normal distribution, inverse-normal distribution and so on are exponential. Then, the probability density (mass) function of Y_k can be generally written as

$$f_{Y_k}(y; \theta, \phi) = c(y, \phi) \exp \left\{ \frac{y\theta - a(\theta)}{\phi} \right\},$$

where $\theta \in \mathbb{R}$ is the canonical parameter and $\phi \in \mathbb{R}^+$ is the dispersion parameter. In this case, we write $Y_k \sim EDF(\theta, \phi)$. The choice of the functions $a(\theta)$ and $c(y, \phi)$ specifies the actual probability function such as gamma and normal distributions. The expectation and variance of Y_k are given by

$$E[Y_k] = a'(\theta),$$

and

$$Var[Y_k] = \phi a''(\theta) = \phi V(E[Y_k]), \quad (5)$$

where $a'(\theta)$ and $a''(\theta)$ are the first and second derivatives of $a(\theta)$ with respect to θ , respectively, and V is the variance function. Table 2 summarizes the probability density functions, the dispersion parameters and the associated variance functions for popular severity distributions.

One useful property of the exponential family is that they are closed under the convolution operation, which yields that the average claim severity given the number of claims, $\bar{Y}|N$, also belongs to the exponential family of distributions with a different dispersion parameter. More specifically, if $Y_k \sim EDF(\theta, \phi)$, then we have $\bar{Y}|N \sim EDF(\theta, \phi/N)$. In particular, the variance of the average severity is given by

$$Var[\bar{Y}|N] = \frac{\phi}{N} V(E[Y_k]) \quad (6)$$

where $V(\cdot)$ is the variance function of the individual severity Y_k .

Severity distributions				
Models	pdf	ϕ	$E[Y]$	$V(\mu)$
Gamma (μ, ϕ)	$\frac{1}{y\Gamma(\nu)} \left(\frac{y}{\mu\nu}\right)^\nu e^{-\frac{\nu}{\mu}y}$	$\frac{1}{\nu}$	μ	μ^2
Inverse Gaussian (μ, ϕ)	$\frac{1}{\sqrt{2\mu y^3\sigma^2}} \exp\left(-\frac{1}{2y} \frac{(y-\mu)^2}{\mu^2\sigma^2}\right)$	σ^2	μ	μ^3
Normal (μ, ϕ)	$\frac{1}{\sqrt{2\pi}\sigma} \exp\left(-\frac{1}{2\sigma^2}(y-\mu)^2\right)$	σ^2	μ	1

Table 2: A summary of severity distributions

Frequency distributions				
Models	\mathcal{I}_N	$M_N(t)$	$M_N^{(1)}(t)$	$M_N^{(2)}(t)$
Binomial	$(-\infty, \infty)$	$\left(1 - \frac{\lambda}{m} + \frac{\lambda}{m}e^t\right)^m$	$\lambda\left(1 - \frac{\lambda}{m} + \frac{\lambda}{m}e^t\right)^{m-1}$	$\frac{\lambda^2(m-1)}{m}\left(1 - \frac{\lambda}{m} + \frac{\lambda}{m}e^t\right)^{m-2}$
Poisson	$(-\infty, \infty)$	$e^{\lambda(e^t-1)}$	$\lambda e^{\lambda(e^t-1)+t}$	$\lambda(\lambda e^t + 1)e^{\lambda(e^t-1)+t}$
ZIP	$(-\infty, \infty)$	$\pi + (1-\pi)e^{\lambda(e^t-1)}$	$(1-\pi)\lambda e^{\lambda(e^t-1)+t}$	$(1-\pi)\lambda(\lambda e^t + 1)e^{\lambda(e^t-1)+t}$
NB	$\left(-\infty, \ln \frac{1}{1-\pi}\right)$	$\left(\frac{\pi}{1-(1-\pi)e^t}\right)^r$	$\frac{\pi r e^t (1-\pi)^t (\ln(1-\pi)+1) (-\frac{\pi}{e^t(1-\pi)^t-1})^{r-1}}{(e^t(1-\pi)^t-1)^2}$	$\frac{r e^t (1-\pi)^t (\ln(1-\pi)+1)^2 (-\frac{\pi}{e^t(1-\pi)^t-1})^r (r e^t (1-\pi)^t + 1)}{(e^t(1-\pi)^t-1)^2}$

Table 3: Moment generating functions and their derivatives for frequency distributions

2.2 Nonlinear and Dependent Model

For the i -th policyholder, we denote by $\mathbf{x}_i = (x_{i1}, \dots, x_{ip})^\top \in \mathbb{R}^p$ the vector of explanatory variables and by t_i the exposure variable. Let N_i be the number of claims during the period t_i , $\{Y_{i,k}\}_{k=1}^{N_i}$ be a sequence of individual claim severity and \bar{Y}_i be the amount of the average severity for the i -th policyholder. The total claim cost is, then, $Z_i = \sum_{k=1}^{N_i} Y_{i,k} = N_i \bar{Y}_i$.

We model that the conditional expectation of N_i given \mathbf{x}_i and t_i is expressed in terms of a regression function $F : \mathbb{R}^p \rightarrow \mathbb{R}$ with the log link function:

$$\ln \lambda_i = \ln \lambda(\mathbf{x}_i, t_i) := \ln \mathbb{E}[N_i | \mathbf{x}_i, t_i] = \ln t_i + F(\mathbf{x}_i) \quad (7)$$

or equivalently, $\lambda_i = t_i \exp\{F(\mathbf{x}_i)\}$.

Following the strategy discussed in Garrido et al. [2016], we incorporate the dependence between frequency and severity by treating N_i as an explanatory variable in a regression model for the conditional expectation of \bar{Y}_i .

We propose that the conditional expectation of \bar{Y}_i given \mathbf{x}_i and N_i is specified by a regression function $S : \mathbb{R}^p \rightarrow \mathbb{R}$ with the log link function:

$$\ln \mu_i = \ln \mu(\mathbf{x}_i, N_i; \gamma) := \ln \mathbb{E}[\bar{Y}_i | \mathbf{x}_i, N_i] = S(\mathbf{x}_i) + \gamma N_i, \quad (8)$$

or equivalently, $\mu_i = \exp \{S(\mathbf{x}_i) + \gamma N_i\}$ where $\gamma \in \mathcal{I}_N$ is the parameter that controls the dependency between frequency and severity, and \mathcal{I}_N is defined in Section 2.1. We assume that γ is constant, which allows us to derive the analytic formulas for the mean and variance of the total claim cost.

It should be highlighted that we do not impose any linearity or other restrictions on $F(\cdot)$ and $S(\cdot)$ as opposed to the GLM framework. Hence, the proposed frequency and severity models given in (7) and (8) are able to represent important information such as nonlinearity and complex interaction in data. The paper uses neural networks to estimate the regression functions $F(\cdot)$ and $S(\cdot)$, which will be discussed in Section 3. Moreover, the NeurFS model is analytically tractable once we have identified the triplet $\{F(\cdot), S(\cdot), \gamma\}$.

An important advantage of our modeling framework is its analytical tractability to provide analytic formulas for mean and variance of the total claim cost as in the traditional GLM. Theorem 1 provides generic formulas for the mean and variance of the total claim cost. For simplicity, we set t_i to be 1.

Theorem 1 *Assume that the moment generating function $M_{N_i}(t)$ for the number of claims is well defined for $t \in \mathcal{I}_{N_i}$, and that the distribution for the average severity is a type of the exponential dispersion family of distributions, i.e., $\bar{Y}_i|N_i \sim EDF(\mu_i, \phi/N_i)$.*

Given the observation \mathbf{x}_i , the mean and variance of the total claim cost are

$$\mathbb{E}[Z_i|\mathbf{x}_i] = e^{S(\mathbf{x}_i)} M_{N_i}^{(1)}(\gamma), \quad (9)$$

and

$$\text{Var}[Z_i|\mathbf{x}_i] = \phi \mathbb{E}[N_i V(\mu_i)|\mathbf{x}_i] + e^{2S(\mathbf{x}_i)} \left(M_{N_i}^{(2)}(2\gamma) - (M_{N_i}^{(1)}(\gamma))^2 \right), \quad (10)$$

for $2\gamma \in \mathcal{I}_{N_i}$ where $M_{N_i}^{(1)}(\cdot)$ and $M_{N_i}^{(2)}(\cdot)$ are the first and second-order derivatives of $M_{N_i}(\cdot)$ defined in (3), and V is the variance function.

Proof: Given \mathbf{x}_i , the mean of the total claim cost S_i is given by

$$\begin{aligned} \mathbb{E}[Z_i|\mathbf{x}_i] &= \mathbb{E}[N_i \bar{Y}_i|\mathbf{x}_i] &= \mathbb{E}[N_i \mathbb{E}[\bar{Y}_i|N_i, \mathbf{x}_i]|\mathbf{x}_i] \\ &= \mathbb{E}\left[N_i e^{S(\mathbf{x}_i) + \gamma N_i}|\mathbf{x}_i\right] \\ &= e^{S(\mathbf{x}_i)} \mathbb{E}\left[N_i e^{\gamma N_i}|\mathbf{x}_i\right] \\ &= e^{S(\mathbf{x}_i)} M_{N_i}^{(1)}(\gamma). \end{aligned}$$

where $M_{N_i}^{(1)}(\gamma)$ is well-defined for $\gamma \in \mathcal{I}_{N_i}$.

From the law of total variance and (5), one calculates that

$$\begin{aligned}
\text{Var}[Z_i|\mathbf{x}_i] &= \mathbb{E}[\text{Var}[Z_i|N_i, \mathbf{x}_i]|\mathbf{x}_i] + \text{Var}(\mathbb{E}[Z_i|N_i, \mathbf{x}_i]|\mathbf{x}_i) \\
&= \mathbb{E}[N_i^2 \text{Var}[\bar{Y}_i|N_i, \mathbf{x}_i]|\mathbf{x}_i] + \text{Var}(N_i \mu_i|\mathbf{x}_i) \\
&= \phi \mathbb{E}[N_i V(\mu_i)|\mathbf{x}_i] + \mathbb{E}[N_i^2 \mu_i^2|\mathbf{x}_i] - \mathbb{E}[N_i \mu_i|\mathbf{x}_i]^2 \\
&= \phi \mathbb{E}[N_i V(\mu_i)|\mathbf{x}_i] + e^{2S(\mathbf{x}_i)} \left(\mathbb{E}[N_i^2 e^{2\gamma N_i}|\mathbf{x}_i] - \mathbb{E}[N_i e^{\gamma N_i}|\mathbf{x}_i]^2 \right) \\
&= \phi \mathbb{E}[N_i V(\mu_i)|\mathbf{x}_i] + e^{2S(\mathbf{x}_i)} \left(M_{N_i}^{(2)}(2\gamma) - (M_{N_i}^{(1)}(\gamma))^2 \right)
\end{aligned}$$

where $M_{N_i}^{(2)}(2\gamma|\mathbf{x})$ given in (3) is well-defined for $2\gamma \in \mathcal{I}_{N_i}$. ■

When marginal distributions for N_i and Y_k are explicitly given, we obtain analytic formulas for the mean and variance of the total claim cost using Theorem 1. Note that Theorem 1 does not hold in general when the individual claim severity distribution does not belong to EDF.

Table 1 and Table 2 summarize popular choices of frequency and severity distributions. In order to explicitly present our framework, we henceforth focus on the case where $N_i \sim ZIP(\lambda_i, \pi)$ and $\bar{Y}_i|N_i \sim Gamma(\mu_i, \phi/N_i)$ without the loss of generality. Here λ_i and μ_i are defined in 7 and 8, and π and ϕ are the associated distribution parameters to be estimated. Under the case, the mean and variance of the total claim cost is given in Example 1.

Example 1 *Suppose that N_i is zero-inflated Poisson with mean λ_i and the proportion of structural zeros π , i.e., $N_i \sim ZIP(\lambda_i, \pi)$ and $Y_i|N_i$ is Gamma with mean μ_i and the dispersion ϕ/N_i , i.e., $Y_i|N_i \sim Gamma(\mu_i, \phi/N_i)$. Then, we have*

$$\mathbb{E}[Z_i|\mathbf{x}_i] = (1 - \pi)\lambda_i \exp\{\lambda_i(e^\gamma - 1) + S(\mathbf{x}_i) + \gamma\} \quad (11)$$

and

$$\begin{aligned}
\text{Var}(Z_i|\mathbf{x}_i) &= \frac{1}{\phi}(1 - \pi)\lambda_i \exp\{2S(\mathbf{x}_i) + \lambda_i(e^{2\gamma} - 1) + 2\gamma\} \\
&\quad + (1 - \pi)\lambda_i(\lambda_i e^{2\gamma} + 1) \exp\{2S(\mathbf{x}_i) + \lambda_i(e^{2\gamma} - 1) + 2\gamma\} \\
&\quad - (1 - \pi)^2 \lambda_i^2 \exp\{2S(\mathbf{x}_i) + 2\lambda_i(e^\gamma - 1) + 2\gamma\}
\end{aligned} \quad (12)$$

Proof: From (9) in Theorem 1 and Table 3, we have

$$\begin{aligned}
\mathbb{E}[Z_i|\mathbf{x}_i] &= e^{S(\mathbf{x}_i)} M_N^{(1)}(\gamma) \\
&= (1 - \pi)\lambda_i \exp\{\lambda_i(e^\gamma - 1) + S(\mathbf{x}_i) + \gamma\}.
\end{aligned}$$

Consider the variance of the total claim cost. Using (10), the variance function of the gamma distribution in Table 2, and the first and second derivatives of M_N in Table 3, we obtain

$$\begin{aligned}
\text{Var}(Z_i|\mathbf{x}_i) &= \phi \mathbb{E}[N_i \mu_i^2] + e^{2S(\mathbf{x}_i)} \left(M_{N_i}^{(2)}(2\gamma) - (M_{N_i}^{(1)}(\gamma))^2 \right) \\
&= \phi e^{2S(\mathbf{x}_i)} M_{N_i}^{(1)}(2\gamma) + e^{2S(\mathbf{x}_i)} \left(M_{N_i}^{(2)}(2\gamma) - (M_{N_i}^{(1)}(\gamma))^2 \right) \\
&= \phi(1-\pi)\lambda_i \exp\{2S(\mathbf{x}_i) + \lambda_i(e^{2\gamma} - 1) + 2\gamma\} \\
&+ (1-\pi)\lambda_i(\lambda_i e^{2\gamma} + 1) \exp\{2S(\mathbf{x}_i) + \lambda_i(e^{2\gamma} - 1) + 2\gamma\} \\
&- (1-\pi)^2 \lambda_i^2 \exp\{2S(\mathbf{x}_i) + 2\lambda_i(e^\gamma - 1) + 2\gamma\}.
\end{aligned}$$

■

It is straightforward to consider γ , π and ϕ to be functions of \mathbf{x}_i . However, we shall assume that they are fixed constants in our analysis to keep our model being parsimonious. Also, it is worth noting that the NeurFS model reduces to a nonlinear independent frequency-severity model when $\gamma = 0$.

3 Neural Networks and Estimation Algorithm

Section 3.1 presents a brief background on neural networks used to estimate the regression functions $F(\cdot)$ and $S(\cdot)$. Then, in Section 3.2, we discuss an algorithm for estimating the triplet $(F(\cdot), S(\cdot), \gamma)$ and the associated distribution parameters (π, ϕ) in the NeurFS model.

3.1 Definitions and Notations

This paper considers feed-forward neural networks to nonparametrically estimate the regression functions of the NeurFS model proposed in Section 2. We first motivate the use of neural networks and then introduce a novel structure of neural networks which is suitable for the NeurFS model.

Simply speaking, the feed-forward neural network is a function approximator, which is constructed by successive compositions of *hidden layers* consisting of affine transformations and non-linear activation functions. In particular, a large volume of empirical studies demonstrates that deep neural networks which uses many hidden layers show better performance than shallower neural networks in approximating a target function on various tasks and data. One of the key reasons for the great success of deep neural networks in practice lies on their universal approximation property, implying that neural networks can approximate any Borel measurable function with arbitrary precision (Hornik et al. [1989], Hornik [1991] and Barron [1993]). In the context of a statistical model based on neural networks, the expressive power of neural networks empowers the statistical model

to represent complex relationships and important interactions among explanatory variables. Consequently, deep learning have been widely adopted to almost all aspects in finance and economics, e.g., predicting abnormal trading behavior, credit default prediction, asset movement [Martinez, 2022, Cheng et al., 2023, Sebastiao and Godinho, 2021, Zhong and Enke, 2019]

The fact that neural networks can efficiently handle high-dimensional data without the curse of dimensionality is another advantage of deep neural networks. In nonparametric regression, this benefit implies that deep neural networks do not depend on the number of explanatory variables and achieve the best approximation to a true function.

In this paper, we consider a two hidden layer feed-forward neural network (TLFN) and modify it for our purpose. Let \mathcal{G}_η be the set of feed-forward neural networks with two hidden layers and η neurons on each layer, which is explicitly given by

$$\begin{aligned} \mathcal{G}_\eta = \{f : \mathbb{R}^p \rightarrow \mathbb{R} | f(\mathbf{x}) = W_3 z + b_3, z = \sigma(W_2 y + b_2), \\ y = \sigma(W_1 \mathbf{x} + b_1), W_1 \in \mathbb{R}^{\eta \times p}, W_2 \in \mathbb{R}^{\eta \times \eta}, W_3 \in \mathbb{R}^{1 \times \eta}, b_1, b_2 \in \mathbb{R}^\eta, b_3 \in \mathbb{R}\}, \end{aligned} \quad (13)$$

where $\mathbf{x} \in \mathbb{R}^p$ is the input vector, W_1 , W_2 and W_3 are the weight parameters, b_1 , b_2 and b_3 are the bias parameters. We denote by $\theta := (W_1, W_2, W_3, b_1, b_2, b_3) \in \mathbb{R}^d$ the parameter of neural networks where $d := \eta(\eta + p + 3) + 1$ is the dimension of the neural network. Note that, throughout the paper, the activation function σ is chosen as the exponential linear unit (ELU) suggested in Clevert et al. [2016]:

$$\sigma(x) = \begin{cases} x & \text{if } x > 0, \\ e^x - 1 & \text{if } x < 0, \end{cases}$$

and is applied element-wise.

3.2 Estimation of $(F(\cdot), S(\cdot), \gamma)$ and Distribution Parameters (π, ϕ)

Suppose that we construct a dataset from m independent observations:

$$\{\mathbf{z}_i\}_{i=1}^m := \{\mathbf{x}_i, n_i, t_i, \bar{y}_i\}_{i=1}^m$$

where $\mathbf{x}_i \in \mathbb{R}^p$ is the vector of explanatory variables, n_i is the number of claims observed for the duration t_i and \bar{y}_i is the average severity for the i -th policyholder.

Recall that the number of claims follows a zero-inflated Poisson distribution and the average severity follows a Gamma distribution. Let $f_N(\cdot; \lambda, \pi)$ be the probability distribution of the zero-inflated Poisson distribution with mean λ and the proportion of structural zeros π , which is given

by

$$f_N(N = n; \lambda, \pi) = \begin{cases} \pi + (1 - \pi)e^{-\lambda}, & n = 0 \\ (1 - \pi)\frac{e^{-\lambda}\lambda^n}{n!}. & n = 1, 2, \dots \end{cases}$$

Given $\{\mathbf{x}_i, n_i, t_i\}_{i=1}^m$, the log-likelihood function for the number of claims is given by

$$\begin{aligned} \ell_N(F, \pi) &= \sum_{i=1}^m \ln f_N(n_i; \lambda_i, \pi) \\ &= \sum_{i=1}^m \ln f_N(n_i; t_i \exp\{F(\mathbf{x}_i)\}, \pi) \\ &= \ell_{N,0}(F, \pi) + \ell_{N,1}(F, \pi) \end{aligned} \quad (14)$$

where $\ell_{N,0}$ is the likelihood function for N_i having zero frequency, i.e., $n_i = 0$, and $\ell_{N,1}$ is the likelihood function for N_i having non-zero frequency, i.e., $n_i > 0$, which are defined as follows:

$$\ell_{N,0}(F, \pi) = \sum_{\{i:n_i=0\}} \ln(\pi + (1 - \pi) \exp\{-t_i \exp(F(\mathbf{x}_i))\}),$$

and

$$\ell_{N,1}(F, \pi) = \sum_{\{i:n_i>0\}} \left(\ln(1 - \pi) - t_i e^{F(\mathbf{x}_i)} + n_i(\ln t_i + F(\mathbf{x}_i)) - \ln(n_i!) \right).$$

Then, the best regression function $F^*(\cdot)$ and the associated distribution parameter π^* in the frequency model can be estimated by minimizing the negative log-likelihood function given in (14) over the class \mathcal{G}_η of TLFNs:

$$\begin{aligned} (F^*, \pi^*) &= \arg \min_{F \in \mathcal{G}_\eta, \pi \in [0,1]} \ell_N(F, \pi) \\ &= \arg \min_{\theta \in \mathbb{R}^d, \pi \in [0,1]} \ell_N(F(\cdot; \theta), \pi) \end{aligned} \quad (15)$$

where \mathcal{G}_η is defined in (13) and $F(\cdot; \theta) \in \mathcal{G}_\eta$ is the two-hidden layer neural network with the parameter θ . We introduce an auxiliary variable $\bar{\pi} \in \mathbb{R}$ such that

$$\pi := \text{sigmoid}(\bar{\pi}) = \frac{1}{1 + e^{-\bar{\pi}}},$$

where $\text{sigmoid}(x)$ is the sigmoid function, so that the range of π is $[0, 1]$. By denoting $\Theta_F = (\theta, \bar{\pi})$, one can convert the constrained optimization problem (15) into an unconstrained optimization problem as follows:

$$(F^*, \bar{\pi}^*) = \arg \min_{\Theta_F \in \mathbb{R}^{d+1}} \ell_N \left(F(\cdot; \theta), \frac{1}{1 + e^{-\bar{\pi}}} \right), \quad (16)$$

and we have $\pi^* = \frac{1}{1+e^{-\bar{\pi}^*}}$.

The proposed neural network architecture for estimating $(F^*, \bar{\pi}^*)$ is illustrated in Figure 2. In practice, stochastic gradient descent (SGD) algorithm or its variants such as ADAM of [Kingma and Ba \[2015\]](#) have been successfully implemented to solve optimization problems involving deep neural networks although, in theory, they are only guaranteed to converge to a local minimum when the objective function is nonconvex.¹ In this paper, the total parameter Θ_F including the parameter of the neural network θ and the distribution parameter π will be estimated using ADAM.

Let $f_{Y|N}(\cdot; \mu, \phi)$ denote the probability density function of the Gamma distribution with mean μ and the dispersion parameter ϕ given by

$$f_{Y|N}(y; \mu, \phi) = \frac{1}{y\Gamma(\phi^{-1})} \left(\frac{y}{\mu\phi}\right)^{\frac{1}{\phi}} e^{-\frac{y}{\mu\phi}}.$$

Given $\{\mathbf{x}_i, n_i, t_i, \bar{y}_i\}_{i=1}^m$, the log-likelihood function for the average severity is written as

$$\begin{aligned} \ell_{\bar{Y}|N}(S, \gamma, \phi) &= \sum_{\{i:n_i>0\}} \ln f_{\bar{Y}|N}\left(\bar{y}_i; \mu_i, \frac{\phi}{n_i}\right) \\ &= \sum_{\{i:n_i>0\}} \ln f_{\bar{Y}|N}\left(\bar{y}_i; \exp\{S(\mathbf{x}_i) + \gamma n_i\}, \frac{\phi}{n_i}\right) \\ &= \sum_{\{i:n_i>0\}} \left(-\ln \bar{y}_i - \ln \Gamma\left(\frac{n_i}{\phi}\right) + \frac{n_i}{\phi} \left(\ln \bar{y}_i + \ln\left(\frac{n_i}{\phi}\right) - (S(\mathbf{x}_i) + \gamma n_i) \right) \right. \\ &\quad \left. - \frac{n_i \bar{y}_i}{\phi} \exp\{-(S(\mathbf{x}_i) + \gamma n_i)\} \right). \end{aligned}$$

Notice that while the paper uses the entire dataset, m independent observations, to compute the log-likelihood function for the frequency in (14), the subset of the dataset for which the number of claims is positive is only used for computing the log-likelihood function for the average severity. We then minimize the log-likelihood function $\ell_{\bar{Y}|N}$ and restrict the regression function $S(\cdot)$ over the set \mathcal{G}_η of TLFNs to estimate (S^*, γ^*, ϕ^*) :

$$\begin{aligned} (S^*, \gamma^*, \phi^*) &= \arg \min_{S \in \mathcal{G}_\eta, \gamma \in \mathbb{R}, \phi > 0} \ell_{\bar{Y}|N}(S, \gamma, \phi) \\ &= \arg \min_{\theta \in \mathbb{R}^d, \gamma \in \mathbb{R}, \phi > 0} \ell_{\bar{Y}|N}(S(\cdot; \theta), \gamma, \phi), \end{aligned} \tag{17}$$

where $S(\cdot; \theta)$ is the TLFN with the parameter θ . The constrained optimization problem (17) can be transformed into an unconstrained optimization problem by introducing an auxiliary variable $\bar{\phi} \in \mathbb{R}$ such that $\phi = e^{\bar{\phi}}$:

$$(S^*, \gamma^*, \bar{\phi}^*) = \arg \min_{\Theta_S \in \mathbb{R}^{d+2}} \ell_{\bar{Y}|N}(S(\cdot; \theta), \gamma, e^{\bar{\phi}}), \tag{18}$$

¹We refer to [Raginsky et al. \[2017\]](#), [Lim et al. \[2021\]](#), [Chau et al. \[2021\]](#), [Lim and Sabanis \[2022\]](#) and [Lim et al. \[2023\]](#) for recent progress on the global convergence of stochastic optimization algorithms in deep learning.

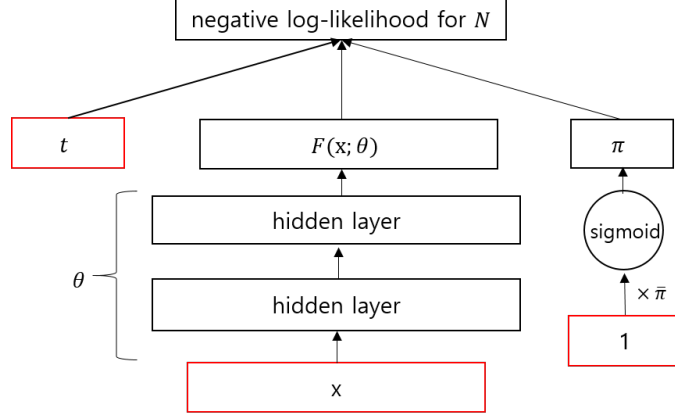


Figure 2: Neural network architecture for the frequency model. The boxes colored in red represent input vectors.

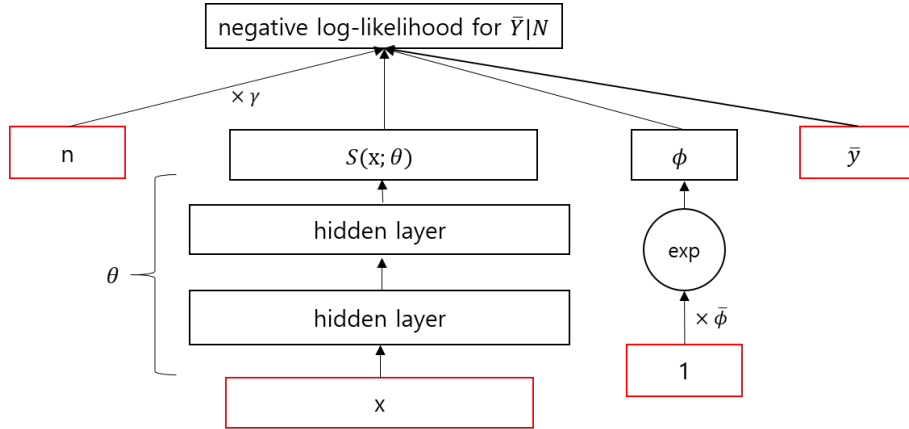


Figure 3: Neural network architecture for the severity model. The boxes colored in red represent input vectors.

where $\Theta_S = (\theta, \gamma, \bar{\phi}) \in \mathbb{R}^{d+2}$ is the total parameter to be estimated for the average severity model. The best dispersion parameter ϕ^* is computed as $e^{\bar{\phi}^*}$. Figure 3 shows the proposed neural network architecture for the average severity model. We also use ADAM to solve the optimization problem (18) involving TLFN.

4 Simulation Study

This section examines the performance of the NeurFS model using an artificial dataset where $(F(\cdot), S(\cdot), \gamma)$ and (π, ϕ) are explicitly known. As a benchmark, we consider two existing models: independent GLM (iGLM) and dependent GLM (dGLM) of Garrido et al. [2016]. iGLM assumes that the regression functions $F(\cdot)$ and $S(\cdot)$ are linear and that frequency and severity are indepen-

dent, while dGLM identifies a linear form of dependence between claim counts and claim sizes, but still imposes a linear restriction on $F(\cdot)$ and $S(\cdot)$.

Let $\mathbf{x}_i = (x_{i1}, x_{i2}) \in \mathbb{R}^2$ be the vector of explanatory variables for the i -th observation. We assume $t_i = 1$ for all observations, and define $F(\mathbf{x}_i) = (x_{i1} - 0.5)^2 + (x_{i2} - 0.5)^2$ and $S(\mathbf{x}_i) = x_{i1}^2 + x_{i2}^2$. Suppose that N_i follows the zero-inflated Poisson distribution with the mean, $\lambda_i := \exp\{F(\mathbf{x}_i)\}$, and the proportion of structured zeros $\pi = 0.2$, and that $\bar{Y}_i|N_i$ follows the Gamma distribution with the mean function, $\mu_i := \exp\{S(\mathbf{x}_i) + \gamma N_i\}$, and the dispersion ϕ/N_i . We set γ to 0.5. Then, from Example 1, the true mean of the total claim cost Z_i is given by

$$E[Z_i|\mathbf{x}_i] = (1 - \pi)\lambda_i \exp\{\lambda_i(e^{0.5} - 1) + S(\mathbf{x}_i) + 0.5\}.$$

We generate 40,000 training samples $\{\mathbf{x}_i, n_i, \bar{y}_i\}_{i=1}^{40,000}$ with $x_{ij} \sim U(\{0, \frac{1}{10}, \frac{2}{10}, \dots, 1\})$ for $j = 1, 2$, so that we have $P(x_{ij} = \frac{k}{10}) = 1/11$ for $k = 0, 1, \dots, 10$. That is, each \mathbf{x}_i is uniformly sampled from the discrete grid, denoted as $\mathcal{X}_1 := \{(x_1, x_2) : x_1, x_2 \in \{0, \frac{1}{10}, \frac{2}{10}, \dots, 1\}\}$. Note that this dataset possesses nonlinear relationships in explanatory variables and dependence structure between the frequency and severity components. Using the dataset, we test the impact of nonlinearity and the dependence on fitting aggregate loss models.

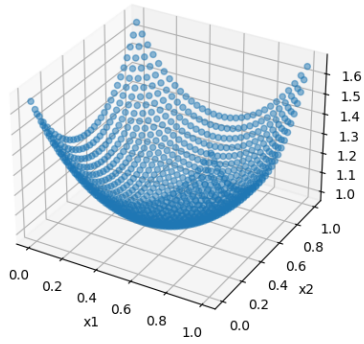
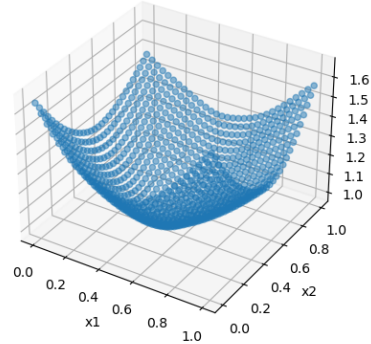
4.1 Frequency Model

For the regression function $F(\cdot)$, we consider TLFN with 25 neurons on each layer. The model is trained using ADAM for 50 epochs with 128 batch size. For ADAM, the paper uses the learning rate of 0.001 and apply the same hyperparameters, $\beta_1 = 0.9$, $\beta_2 = 0.999$ and $\epsilon = 10^{-8}$, as suggested in Kingma and Ba [2015] to solve the optimization problem (16).

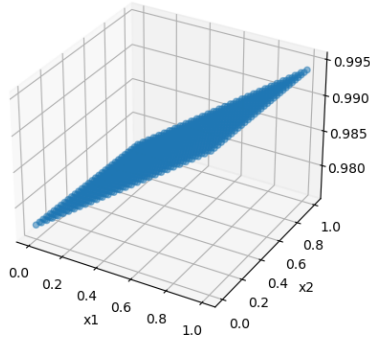
We define a test grid to evaluate the performance of models:

$$\mathcal{X}_2 := \left\{ (x_1, x_2) : x_1, x_2 \in \left\{ 0, \frac{1}{30}, \dots, 1 \right\} \right\},$$

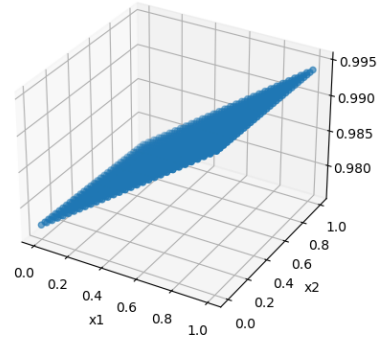
which is finer than the training grid \mathcal{X}_1 . Figure 4 shows that the true mean function $\exp(F(\cdot))$ and the estimated functions $\exp(\hat{F}(\cdot))$ which are obtained from the NeurFS model, iGLM and dGLM on the test grid \mathcal{X}_2 . It is clearly observed that the NeurFS model recovers the nonlinear true mean function accurately. In contrast, iGLM and dGLM completely fail to fit the true function due to their linear assumption on the regression function $F(\cdot)$. Note that the frequency components of iGLM and dGLM are treated in the exactly same manner, so they produce same predicted curves for estimating the mean function of claim counts. As the true regression function $F(\cdot)$ is explicitly known, the paper uses mean absolute error (MAE) and root mean squared error (RMSE) of each model for $F(\cdot)$ as performance measures, that compute L_1 and L_2 norm of the prediction error on

(a) True $\exp\{F(\cdot)\}$ 

(b) NeurFS



(c) GLM



(d) dGLM

Figure 4: Predicted curves for $\exp(F)$ of the frequency model.

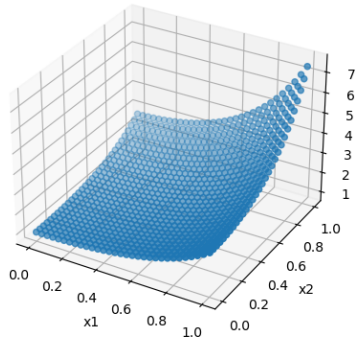
the test grid \mathcal{X}_2 , respectively:

$$MAE = \frac{1}{961} \sum_{i=0}^{30} \sum_{j=0}^{30} |F((u_i, u_j)) - \hat{F}((u_i, u_j))|, \quad (19)$$

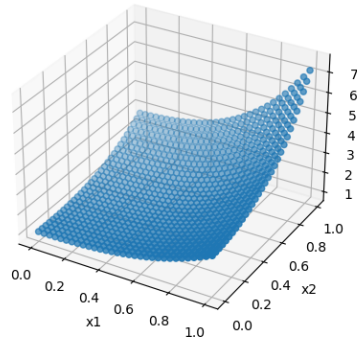
$$RMSE = \sqrt{\frac{1}{961} \sum_{i=0}^{30} \sum_{j=0}^{30} |F((u_i, u_j)) - \hat{F}((u_i, u_j))|^2}, \quad (20)$$

where $u_i = \frac{i}{30}, i = 0, 1, \dots, 30$. As shown in Table 4, the MAE and RMSE of the NeurFS are significantly lower than that of iGLM and dGLM.

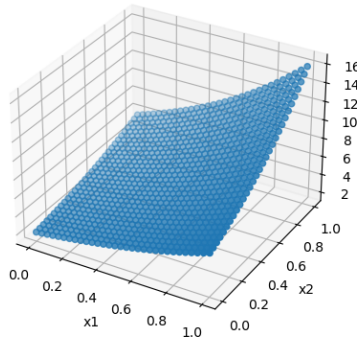
Let $\hat{\pi}$ denote the predicted probability of structural zeros for the zero-inflated Poisson distribution. Figure 7 plots the trajectory of $\hat{\pi}$ estimated by the NuerFS model during the training phase. The value of the estimate $\hat{\pi}$ starting at about 0.06 quickly converges to the true value of 0.2 after



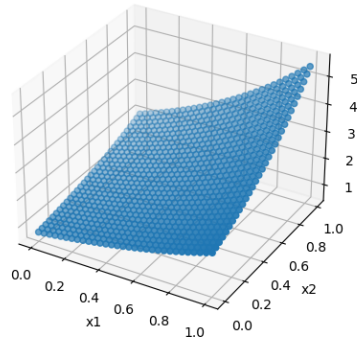
(a) True $\exp\{S(\cdot)\}$



(b) NeurFS



(c) GLM



(d) dGLM

Figure 5: Predicted curves for $\exp(S(\cdot))$ of the average severity model.

around 10 epochs. On the other hands, according to Table 4, iGLM and dGLM overestimate π to compensate the nonlinearity of the true target function, which leads to a large prediction error.

4.2 Severity Model

Let us focus on the severity model including $S(\cdot)$ and γ defined in (8), and the dispersion parameter ϕ . As done in the frequency model, TLFN with 25 neurons on each hidden layer is trained for 50 epochs with 128 batch size. We then obtain the estimates $(\hat{S}(\cdot), \hat{\gamma}, \hat{\phi})$ by solving (17) using ADAM with the same hyperparameters in the frequency model.

We first discuss approximations to $S(\cdot)$ from the NeurFS model, iGLM and dGLM by comparing them with the true target function $\exp(S(\cdot))$ on the test grid \mathcal{X}_2 . As seen in Figure 5, the NeurFS

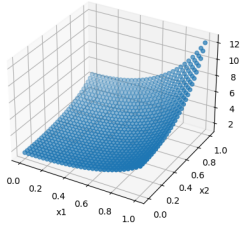
model perfectly replicates the true function. However, iGLM and dGLM provide substantially biased curves and the errors become prominent when x_1 and x_2 are close to 1.

It is also important to understand the behavior of the fitted curves with respect to claim counts, as the mean of the average severity is dependent on the number of claims. Figure 6 displays the true mean functions $\mu(\cdot, k; \gamma)$, which is equivalent to $\exp\{S(\cdot) + \gamma k\}$, for $k = 1, 2, 3$ and their estimated functions of the NeurFS, iGLM and dGLM. Looking at the curves of iGLM, see (g), (h) and (i) in Figure 6, the predictions remain unchanged regardless of k due to the independence between frequency and severity. This misspecification of the dependence structure results in overestimating (underestimating) the mean of the average severity when k is small (large). While dGLM shows improved performance by capturing the positive dependence between the frequency and severity components, its prediction errors are still significant across all k . On the other hand, Figure 6 (d), (e), (f) demonstrate the ability of the NeurFS to recover nonlinear regression functions and the dependence of the aggregate claims process. Table 4 reports the MAE and RMSE of each model for the mean of the average severity, which are similarly calculated as in (19) and (20) on the test grid, and the estimates $\hat{\gamma}$ and $\hat{\phi}$. The numerical results indicate that the NeurFS significantly outperforms iGLM and dGLM in terms of the MAE and RMSE, and our model accurately estimates the level of the dependence γ and the associated distribution parameter ϕ . The convergence pattern of $\hat{\gamma}$ and $\hat{\phi}$ is illustrated in Figure 7.

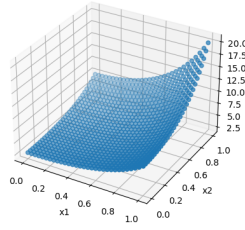
Remark 1 We also test the performance of an independent NeurFS model with $\gamma = 0$ to investigate the effectiveness of γ by removing n_i to predict μ_i . While this model captures nonlinear interactions among input features \mathbf{x} , it cannot incorporate the dependence between the frequency and severity components. In other words, it represents a nonlinear version of the dGLM. The MAE and RMSE in estimating the total claim cost for the independent NeurFS model are 0.7567 and 0.8330, respectively. Compared to the results in Table 4, the independent NeurFS model is inferior to our NeurFS model, which accounts for γ . This demonstrates that γ is crucial in accurately estimating the total claim cost in NeurFS models. ■

4.3 Total Claim Cost

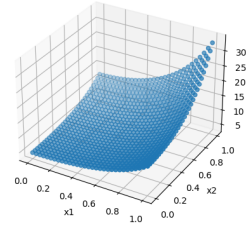
Based on the fitted frequency and severity components of the NeurFS model, we are able to predict the mean of the total claim cost using (11), which is the main purpose of the aggregate claims model. We compute the MAE and RMSE of prediction error of each model on the test grid and summarize the results in Table 4. Moreover, Figure 8 provides the true mean function of the total claim cost and the predicted curves by the NeurFS, iGLM and dGLM. As expected, the NeurFS



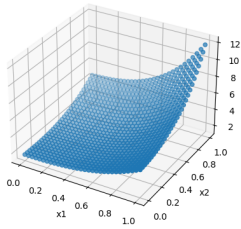
(a) True $\mu(\cdot, k; \gamma)$ with $k = 1$



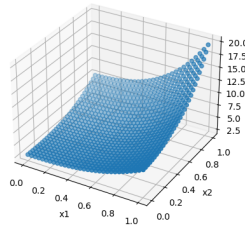
(b) True $\mu(\cdot, k; \gamma)$ with $k = 2$



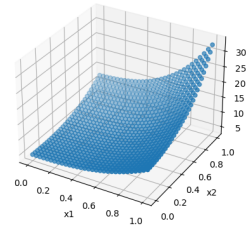
(c) True $\mu(\cdot, k; \gamma)$ with $k = 3$



(d) NeurFS with $k = 1$

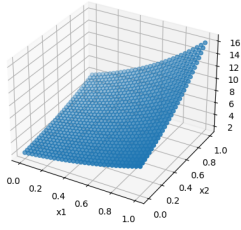


(e) NeurFS with $k = 2$

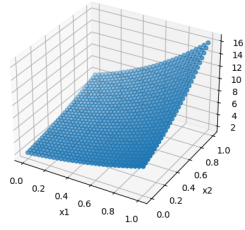


(f) NeurFS with $k = 3$

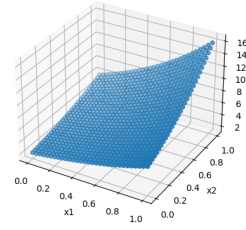
GLM



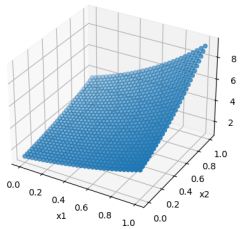
(g) iGLM with $k = 1$



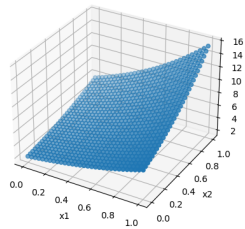
(h) iGLM with $k = 2$



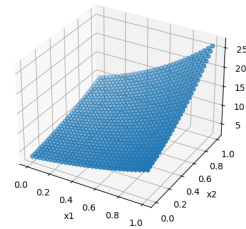
(i) iGLM with $k = 3$



(j) dGLM with $k = 1$



(k) dGLM with $k = 2$



(l) dGLM with $k = 3$

Figure 6: Predicted curves for $\mu(\cdot, k; \gamma)$ by the NeurFS, iGLM and dGLM for $k = 1, 2, 3$. Note that $\mu(\cdot, k; \gamma) = \exp\{S(\cdot) + \gamma k\}$ by the definition of (8).

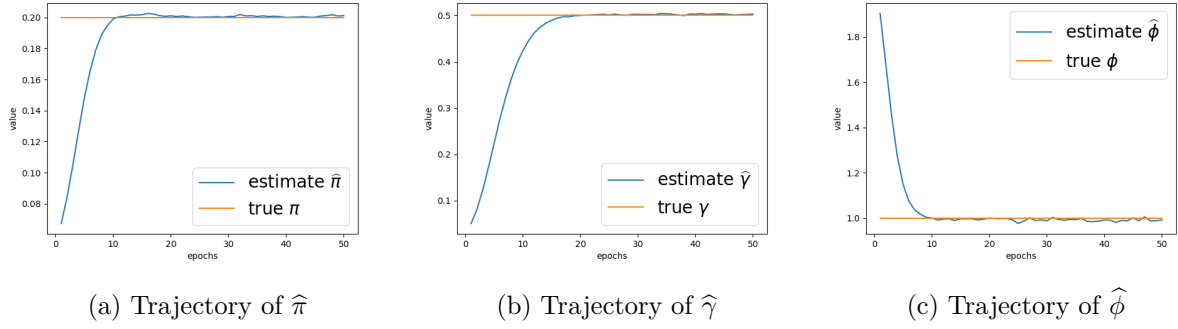


Figure 7: Approximation to π , γ and ϕ by the NeurFS model ($p = 2$).

achieves the lowest MAE and RMSE, 0.0912 and 0.1159, respectively, which are approximately from 2% to 4% of the prediction errors of the iGLM and dGLM. The remarkable results demonstrate that our proposed model is effectively able to extract nonlinear relation in explanatory variables and capture dependence between the claim counts and severity. Furthermore, we find that the impact of model misspecification can bring substantial prediction errors when dealing with the aggregate claims data.

4.4 Performance under the $p = 100$ case

We conduct a similar experiment, but with $p = 100$, to demonstrate that the NeurFS estimates π , γ , and ϕ in high-dimensional cases. Specifically, let $\mathbf{x}_i = (x_{i1}, x_{i2}, \dots, x_{i100})$ for the i -th observation. We define:

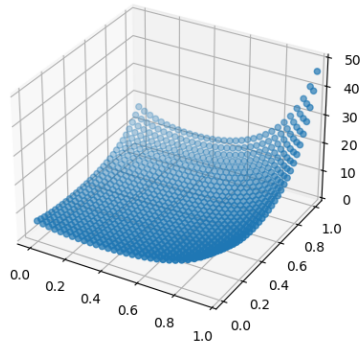
$$F(\mathbf{x}_i) = \sum_{j=1}^{100} (x_{ij} - 0.5)^2, \quad \text{and} \quad S(\mathbf{x}_i) = \sum_{j=1}^{100} x_{ij}^2.$$

Assume that N_i follows the zero-inflated Poisson distribution with mean, $\lambda_i := \exp\{F(\mathbf{x}_i)\}$, and the proportion of structured zeros $\pi = 0.25$. Additionally, given N_i , \bar{Y}_i follows the Gamma distribution with the mean function $\mu_i := \exp\{S(\mathbf{x}_i) + \gamma N_i\}$ and the dispersion ϕ/N_i where $\gamma = 0.3$ and $\phi = 1$.

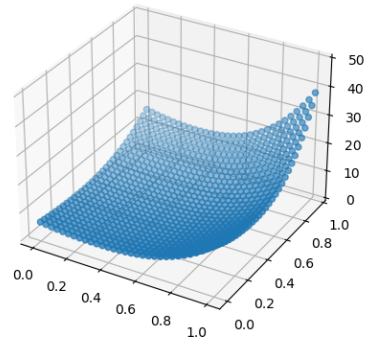
For training neural networks, we use 1,000,000 samples $\{\mathbf{x}_i, n_i, \bar{y}_i\}_{i=1}^{1,000,000}$, where x_{ij} is drawn from a uniform distribution $U(\{0, \frac{1}{10}, \frac{2}{10}, \dots, 1\})$ for $j = 1, 2, \dots, 100$. Figure 9 clearly indicates that the NeurFS can accurately estimate π , γ , and ϕ with $p = 100$.

Table 4: A summary of results of iGLM, dGLM and the NeurFS for estimating frequency, average severity, and the total claim cost. The true value of π is 0.2, and the true values of γ and ϕ are 0.5 and 1, respectively. NA means “not applicable”.

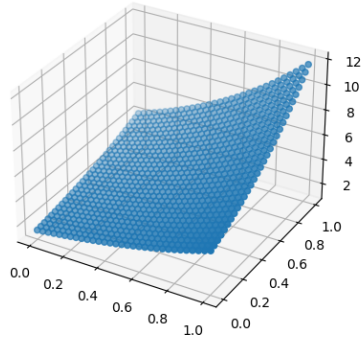
Model	GLM	dGLM	NeurFS
Frequency			
MAE	0.2167	0.2167	0.1513
RMSE	0.2572	0.2572	0.1894
$\hat{\pi}$	0.2591	0.2591	0.2007
Average severity			
MAE	4.1135	0.2065	0.0319
RMSE	4.4662	0.2867	0.0394
$\hat{\gamma}$	NA	0.5190	0.5022
$\hat{\phi}$	2.1888	1.0300	0.9915
Total claim cost			
MAE	3.3289	2.7832	0.0912
RMSE	5.1093	4.5908	0.1159



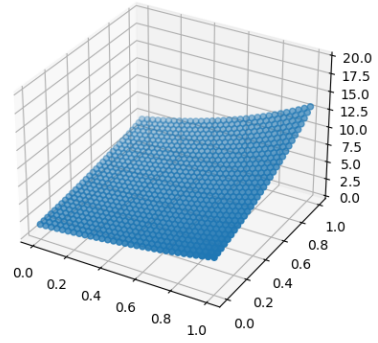
(a) True $\exp\{S(\cdot)\}$



(b) NeurFS

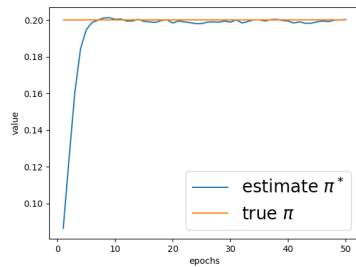


(c) iGLM

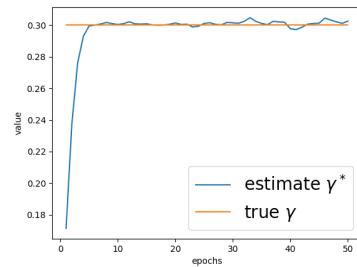


(d) dGLM

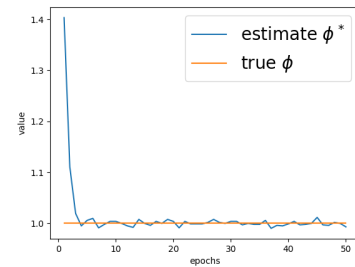
Figure 8: Predicted curves for the total claim cost.



(a) Trajectory of $\hat{\pi}$



(b) Trajectory of $\hat{\gamma}$



(c) Trajectory of $\hat{\phi}$

Figure 9: Approximation to π , γ and ϕ by the NeurFS model ($p = 100$).

5 Application to Insurance Claims

This section is devoted to applying our proposed model to real insurance claims data. This empirical study shows the feasibility and effectiveness of the NeurFS model in practice.

5.1 Data Description

We consider a French insurance claims dataset where 668,436 samples are recorded. Each sample includes 9 explanatory variables $\mathbf{x}_i \in \mathbb{R}^9$, the number of claims n_i , the average severity \bar{y}_i , exposure t_i (year) and the total claim cost z_i for the exposure period. Our goal is to predict the total claim cost z_i , that is, $n_i \bar{y}_i$, given the characteristics \mathbf{x}_i and the exposure t_i of an individual driver. We refer to Table 5 for the description of explanatory variables.

Table 5: Explanatory variables and their description. In the second column, ‘C’ and ‘N’ represent categorical and numerical variables, respectively.

Variable	Type	Description
VehPower	C	The power of the car (6 classes)
VehAge	C	The vehicle age in years. $((0,1], (1,4], (4,10], (10, \infty))$
DrivAge	C	The driver age in years $([18,21], (21,25], (25,35], (35,45], (45,55],(55,70], (70,\infty))$
VehBrand	C	The car brand (14 classes)
VehGas	C	The car gas (diesel or regular)
Region	C	The policy region in France (22 classes)
Area	C	The density value of the city community where the car driver lives in (6 classes)
Density	N	the density of inhabitants in the city the driver of the car lives in
BonusMalus	N	Bonus/malus, between 50 and 350 : < 100 means bonus, > 100 means malus in France.

Table 6 provides the empirical distribution of claim counts and the average severity in each of the claim count. In this dataset, 96.33% of policyholders have never requested a claim, whereas only 3.67% of policy records have positive claim counts. This observation leads to the zero-inflated distribution of the total claim amounts as shown in the left panel of Figure 1. Moreover, Figure 10 illustrates the distribution of average claim amounts is highly skewed to the right. As a result,

Table 6: A summary of claim counts and average severity of auto insurance claims.

Claim count	% of observations	Average severity
0	96.33	0
1	3.52	2177.12
2	0.13	3631.73
3	0.01	2213.63
> 4	< 0.01	2735.04

the distribution of the total claim amounts is not only zero-inflated, but also right-skewed, which motivates the introduction of two-part models.

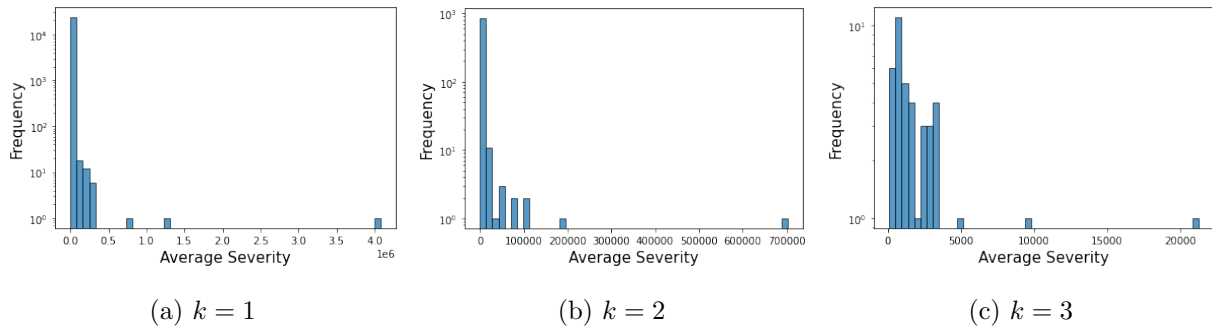


Figure 10: Histograms of average claim amounts given that claim count is $k \in \{1, 2, 3\}$. Note that y-axis uses log scale.

The data is equally split into a training set to train models and a test set to evaluate the trained model. Categorical variables are converted to dummy variables using one-hot encoding and max-min normalization is used to scale numerical variables. As in Section 4, we compare the performance of the NeurFS model with that of two GLM based models, namely iGLM and dGLM. For the GLM approaches, we additionally include an intercept variable.

5.2 Evaluation Metrics

In the synthetic dataset in Section 4 where target regression functions are explicitly known, we used MAE and RMSE to evaluate the performance of predictive models. However, when we consider real-world data, a careful consideration has to be made in choosing evaluation metrics to assess the quality of models, as the target regression functions are no longer available explicitly.

learning rate	(0.01, 0.001)
batch size	(256, 512, 1024)
the number of neurons	(50, 100)
the number of epochs	100

Table 7: Hyperparameters used to train the NeurFS models. Total 12 configurations of hyperparameters are tested.

Suppose that the NeurFS model, iGLM and dGLM are calibrated based on the training set. Denote predictions of each model for frequency, average severity and the total claim amount by \hat{n}_i , \hat{y}_i and \hat{z}_i , respectively, for $i = 1, \dots, N'$ where N' is the number of samples in the training (test) set. To examine the fitted frequency models, we compute mean Poisson deviance (MPD):

$$MPD = \frac{1}{N'} \sum_{i=0}^{N'} 2 \left(n_i \log \left(\frac{n_i}{\hat{n}_i} \right) + \hat{n}_i - n_i \right),$$

which is widely used to describe goodness of fit for Poisson regression. For the severity parts, we continue to consider MAE and RMSE to measure the difference between the actual average severity and the predicted average severity.

Due to the nature of the zero-inflated and right-skewed distribution of total claim amount, which is confirmed in Figure 1, the use of MAE and RMSE as evaluation metrics leads to misleading interpretation of prediction results. An alternative way is to compute a Gini index of the ordered Lorenz curve, proposed in [Frees et al. \[2011b\]](#), which compares the ability of a base model and a competing model for risk classification. We refer to [Frees et al. \[2011b\]](#) for detailed analysis and properties of the Gini index in insurance ratemaking.

5.3 Results of Analysis

We calibrate the NeurFS model using TLFNs defined in (13). To tune the neural networks, we investigate different hyperparameters summarized in Table 7. That is, for each TLFN, we test 12 different hyperparameter configurations and then report the best model that achieves the lowest NLL on the test set. We repeat all the experiments three times with different random splits to obtain the mean and standard deviation of evaluation metrics.

Table 8 provides MDPs of the frequency models estimated from three models, i.e., iGLM, dGLM and NeurFS, which is computed on the training set and test set. As iGLM and dGLM share the common frequency part, their performance measures are identical. We find that the NeurFS model

Evaluation metrics	dataset	iGLM	dGLM	NeurFS
MPD	training set	0.2349 (0.0004)	0.2349 (0.0004)	0.2258 (0.0011)
	test set	0.2356 (0.0004)	0.2356 (0.0004)	0.2318 (0.0003)

Table 8: The averaged MPD and their standard deviations of iGLM, dGLM and NeurFS on the training set and test set for the frequency model. The numbers in parentheses indicate the standard deviations calculated from three different random data splits.

Evaluation metrics	dataset	iGLM	dGLM	NeurFS
MAE	training set	1861.7 (31.0)	1621.5 (33.6)	1488.7 (22.4)
	test set	1877.4 (27.3)	1637.4 (32.9)	1516.0 (19.6)
RMSE	training set	2970.5 (362.1)	2803.3 (568.8)	2737.6 (383.1)
	test set	7817.0 (125.92)	7763.8 (51.9)	7733.5 (130.4)

Table 9: The averaged evaluation metrics and their standard deviations of iGLM, dGLM and NeurFS on the training set and test set for the severity model. The numbers in parentheses indicate the standard deviations calculated from three different random data splits.

achieves lower MDP than GLM based approaches on both training set and test set, implying that the proposed model has better fitting and predictive performance than iGLM and dGLM.

Table 9 reports the estimation results of each model for the averaged severity on the training set and test set. Based on the fact that dGLM always outperforms iGLM across all evaluation metrics and datasets, we find that the consideration of the dependence in dGLM leads to large improvements in fitting and predicting the average severity. In addition, the NeurFS model further reduces prediction errors, measured by MAE and RMSE, compared to dGLM by a significant amount. Therefore, the results confirm the dependence and nonlinearity captured by the NeurFS model are crucial for an accurate fit of the insurance claims data.

Lastly, we examine the performance of three different predictive models on the estimation of the total claim cost. By computing the Gini index of the ordered Lorentz curve, a systematic comparison between two predictive models (a base model and a competing model) can be made. Informally, the Gini index quantifies benefits when a base model is replaced by a competing model. A large Gini index implies that the competing model is superior to the base model in estimating the total claim cost and classifying risk groups given a portfolio of policies. We compute all possible pairs of the Gini indices by alternatively selecting the base model and the competing model among

Base score	Alternative score		
	iGLM	dGLM	Neural FS
iGLM	-	0.93	25.79
dGLM	1.48	-	25.75
Neural FS	2.72	8.35	-

Table 10: The averaged Gini indices of iGLM, dGLM and NeurFS model, which are computed from three different random data splits.

iGLM, dGLM and the NeurFS. The numerical results are summarized in Table 10. We find that the NeurFS model as the competing model gets relatively large Gini indices against iGLM and dGLM as the base model. Furthermore, when the NeurFS is chosen as the base model, the Gini index of iGLM and dGLM is relatively small. More concretely, the best model can be determined through a “mini-max” strategy proposed in [Frees et al. \[2014\]](#), which selects the base model that has the smallest of the maximal Gini indices over competing models. For example, when the base model is iGLM, the maximum Gini index is 25.79 achieved by the NuerFS as the competing model. Similarly, the maximal Gini index is 25.48 when the base model is dGLM, and is 8.35 when the base model is the NeurFS. This implies that the NeurFS model has the smallest maximum Gini index. Therefore, the NuerFS model is the best model in terms of the Gini index, which is the least vulnerable to other competing models. These empirical results support the effectiveness of the NuerFS model in practice.

In summary, the numerical results show that the proposed model outperforms iGLM and dGLM in predicting claim frequency using the MPD metric. It also exhibits superior performance in terms of MAE and RMSE when predicting average severity. To evaluate the performance of models in predicting total claims, the paper uses the Gini index, derived from the ordered Lorenz curve, to rank policyholders based on their risk levels. By plotting cumulated claims and ranking policyholders from safest to riskiest based on model predictions, we can visualize the distribution of observed total cumulated claims. In this context, we find that our model excels in ranking the risk level of policyholders by accurately predicting the total claim cost. This enables insurers to charge fair insurance premiums and avoid the adverse selection issue.

5.4 Model interpretation

Due to the ‘black box’ nature of neural networks, we consider a useful tool for explaining the outputs of neural networks based on the Shapely value. The Shapley value, proposed by [Shapley \[1953\]](#),

is a fundamental concept in cooperative game theory for explaining the marginal contributions of players. Given a set of players \mathcal{N} , a cooperative game is characterized by a finite set $\mathcal{S} \subseteq \mathcal{N}$ and a characteristic function $v : \mathcal{P}(\mathcal{S}) \rightarrow \mathbb{R}$ with $v(\emptyset) = 0$ where $\mathcal{P}(\mathcal{S})$ is the set of all possible subset of \mathcal{S} . Simply put, v maps to the sum of payoffs that can be obtained from given players. Then, the Shapely value is given by

$$\phi_i = \sum_{\mathcal{S} \subseteq \mathcal{N} \setminus \{i\}} \frac{|\mathcal{S}|!(|\mathcal{N}| - |\mathcal{S}| - 1)!}{|\mathcal{N}|!} (v(\mathcal{S} \cup \{i\}) - v(\mathcal{S})).$$

Lundberg and Lee [2017] proposed the Shapley additive explanation (SHAP) to interpret predictions of highly complex models such as neural networks, Gradient Boost, XGBoost, by combining local explanation models of Riberiro et al. [2016] with Shapley values. In their seminal work, it is shown that SHAP provides unique additive feature importance values that satisfy three desirable properties: local accuracy, missingness, and consistency. Also, it is proven that SHAP values are more consistent with human intuition than other methods such as the dependence plot, the feature importance and saliency map in the literature. We refer interested readers to Lundberg and Lee [2017] and Adebayo et al. [2018].

In SHAP, each player is considered as an input variable in the model and $v(\cdot)$ is the output of the model of interest. SHAP specifies the explanation model g defined as

$$g(x') = \phi_0 + \sum_{i=1}^{|\mathcal{N}|} \phi_i \tag{21}$$

where $\phi_i \in \mathbb{R}$ is the importance of a input variable i and ϕ_0 , so called the base value, is the prediction value without any features. That is, SHAP value ϕ_i represents the contribution of each feature to the prediction. We build two SHAP models for $F^*(\cdot)$ and $S^*(\cdot)$.

First, we investigate the global importance of each feature, computed by the mean absolute value of that feature over given samples. Figure 11 shows the global feature importance of the 9 explanatory variables for the frequency and severity models. It is observed that significant variables for the frequency and severity models are completely different. For example, BonusMalus is the most influential variable for the frequency model, which is intuitive since BonusMalus, also known as the no-claim discount, is directly determined by the driver’s claim history. More importantly, this indirectly verifies that a driver with a low BonusMalus is likely to avoid car accidents due to skill or defensive driving, justifying the BonusMalus system. Next, the age of the driver is recognized as an important variable in the frequency model, with the impact of the driver’s age being the second most influential for explaining the predicted frequency. LogDensity, Area, and Region are the three most relevant variables for the severity model, consistent with the general consensus that the risk of fatal injury in rural areas is less than in urban areas (Castro-Nuno and Arevalo-Quijada [2018]).

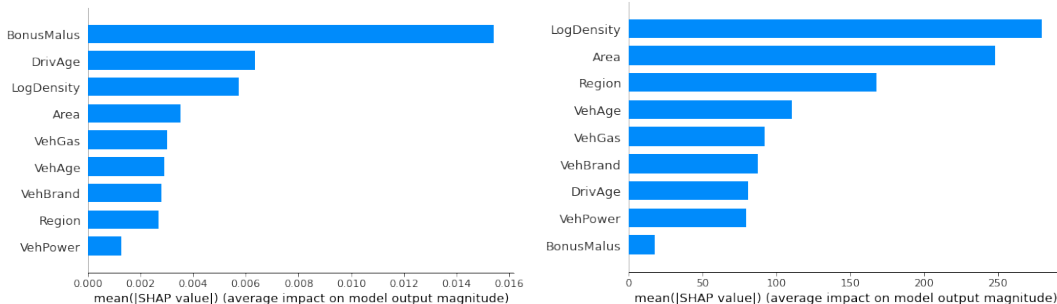


Figure 11: Global feature importance plots for frequency (Left) and severity (Right).

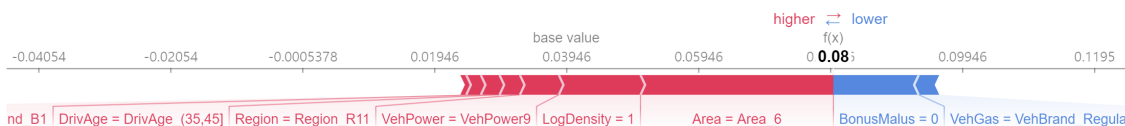


Figure 12: Individual risk profile for the frequency model

Conversely, BonusMalus is the least important factor for severity, as it is a quantity conditional on the occurrence of an accident.

We now perform an individual risk analysis by examining SHAP values for each observation's prediction. Imagine a sample is randomly chosen. We then compute SHAP values for the frequency model, with the model's output being approximately 0.08. Figure 12 illustrates how SHAP values for each feature contribute to the model's output. The base value ϕ_0 , defined in (21), is 0.03946, which is the predicted frequency without any information on the features of the observation. To reach the model's prediction of 0.08, SHAP values of all features are added. In this example, the fact that the driver lives in Area6 increases the frequency rate, while the predicted value is negatively associated with the driver's BonusMalus.

6 Conclusion

This work discusses the challenges in estimating total claim costs in insurance, which are characterized by zero-inflated and right-skewness. We contribute to the advancement of statistical and actuarial science by integrating modern machine learning techniques with an emphasis on dependency modeling. In addition, we offer a practical solution for improving the accuracy of total claim cost estimation in the insurance industry. The superiority of the NeurFS model is confirmed by a synthetic data and real-world insurance claims data.

This scalable and tractable model class can be an important alternative to the traditional GLM in insurance business where a large volume of data is available. In particular, our research output

will contribute to maintaining the competitiveness of an insurer by predicting insurance claims accurately, and avoiding adverse selection. Lastly, we emphasize that the scope of applications of the proposed model is not limited to the insurance claim prediction. It can be applied to analyzing operations loss, health care expenditures or credit assessment data where a joint distribution of frequency and severity is involved. Possible applications include hedging effectiveness of insurance [Wang and Lee \[2023\]](#).

References

- J. Adebayo, J. Gilmer, M. Muelly, I. Goodfellow, M. Hardt, and B. Kim. Sanity checks for saliency maps. *Working paper*, 2018.
- A. Barron. Universal approximation bounds for superpositions of a sigmoidal function. *IEEE Transactions on Information theory*, 39:930–945, 1993.
- E. Brechmann, C. Czado, and S. Paterlini. Flexible dependence modeling of operational risk losses and its impact on total capital requirements. *Journal of Banking & Finance*, 40:271–285, 2014.
- M. Castro-Nuno and M. Teresa Arevalo-Quijada. Assessing urban road safety through multidimensional indexes: Application of multicriteria decision making analysis to rank the spanish provinces. *Transport policy*, 68, 2018.
- H. N. Chau, É. Moulines, M. Rásonyi, S. Sabanis, and Y. Zhang. On stochastic gradient Langevin dynamics with dependent data streams: the fully non-convex case. *SIAM Journal on Mathematics of Data Science*, 3(3):959–986, 2021.
- L.-C. Cheng, W.-T. Lu, and B. Yeo. Predicting abnormal trading behavior from internet rumor propagation: a machine learning approach. *Financial Innovation*, 9(1), 2023.
- D-A. Clevert, T. Unterthiner, and S. Hochreiter. Fast and accurate deep network learning by exponential linear units (elus). *International Conference on Learning Representations(ICLR)*, 2016.
- C. Czado, R. Kastenmeier, E. C. Brechmann, and A. Min. A mixed copula model for insurance claims and claim sizes. *Scandinavian Actuarial Journal*, 4, 2012.
- H. Dahren and G. Dionne. Scaling models for the severity and frequency of external operational loss data. *Journal of Banking & Finance*, 34(7), 2010.
- E. W. Frees, J. Gao, and M. A. Rosenberg. Predicting the frequency and amount of health care expenditures. *North American Actuarial Journal*, 15(3):377–392, 2011a.

- E. W. Frees, G. Meyers, and A. D. Cummings. Summarizing insurance scores using a gini index. *Journal of the American Statistical Association*, 106(495):1085–1098, 2011b.
- E. W. Frees, G. Meyers, and A. D. Cummings. Insurance ratemaking and a gini index. *Journal of Risk and Insurance*, 81(2):335–366, 2014.
- J. Garrido, C. Genest, and J. Schulz. Generalized linear models for dependent frequency and severity of insurance claims. *Insurance: Mathematics and Economics*, 70:205–215, 2016.
- S. Gschlößl and C. Czado. Spatial modelling of claim frequency and claim size in non-life insurance. *Scandinavian Actuarial Journal*, 3:202–225, 2007.
- L. Guelman. Gradient boosting trees for auto insurance loss cost modeling and prediction. *Expert Systems with Applications*, 39:3659–3667, 2012.
- K. Hornik. Approximation capabilities of multilayer feedforward networks. *Neural Networks*, 4: 251–257, 1991.
- K. Hornik, M. Stinchcombe, and H. White. Multilayer feedforward networks are universal approximators. *Neural Networks*, 2:359–366, 1989.
- Y. Huang and S. Meng. Automobile insurance classification ratemaking based on telematics driving data. *Decision Support Systems*, 127, 2019.
- M. Kelly and N. Nielson. Age as a variable in insurance pricing and risk classification. *The Geneva Papers on Risk and Insurance-Issues and Practice*, 31(2):212–232, 2006.
- D. Kingma and J. Ba. Adam: A method for stochastic optimization. *International Conference on Learning Representations (ICLR)*, 2015.
- N. Kramer, E. Brechmann, D. Silversrini, and C. Czado. Total loss estimation using copula-based regression models. *Insurance: Mathematics and Economics*, 53:829–839, 2013.
- D.-Y. Lim and S. Sabanis. Polygonal Unadjusted Langevin Algorithms: Creating stable and efficient adaptive algorithms for neural networks. *arXiv preprint arXiv:2105.13937*, 2022.
- D.-Y. Lim, A. Neufeld, S. Sabanis, and Y. Zhang. Non-asymptotic estimates for TUSLA algorithm for non-convex learning with applications to neural networks with ReLU activation function. *arXiv preprint arXiv:2107.08649*, 2021.
- D.-Y. Lim, A. Neufeld, S. Sabanis, and Y. Zhang. Langevin dynamics based algorithm e-theopoula for stochastic optimization problems with discontinuous stochastic gradient. *arXiv preprint arXiv:2210.13193*, 2023.

- S. Lundberg and S. Lee. A unified approach to interpreting model predictions. *Advances in neural information processing systems(NeurIPS)*, 2017.
- A. Alonso Robisco, J. M. C. Martinez. Measuring the model risk-adjusted performance of machine learning algorithms in credit default prediction. *Financial Innovation*, 8(1), 2022.
- P. Radanliev and D. D. Roure. New and emerging forms of data and technologies: Literature and bibliometric review. *Multimedia Tools and Applications*, 82:2887–2911, 2023.
- M. Raginsky, A. Rakhlin, and M. Telgarsky. Non-convex learning via stochastic gradient Langevin dynamics: a nonasymptotic analysis. *Conference on Learning Theory*, 2017.
- M. T. Riberiro, S. Singh, and C. Guestrin. Why should i trust you?: Explaining the predictions of any classifier. *22nd ACM SIGKDD International Conference on Knowledge Discovery and Data Mining*, pages 1135–1144, 2016.
- H. Sebastiao and P. Godinho. Forecasting and trading cryptocurrencies with machine learning under changing market conditions. *Financial Innovation*, 7(1), 2021.
- L. Shapley. A value for n-person games. *Contributions to the Theory of Games*, 2:307–317, 1953.
- P. Shi, X. Feng, and A. Ivantsova. Dependent frequency-severity modeling of insurance claims. *Insurance: Mathematics and Economics*, 64:417–428, 2015.
- X. Su and M. Bai. Stochastic gradient boosting frequency-severity model of insurance claims. *PloS one*, 15, 2020.
- J. Urbina and M. Guillén. An application of capital allocation principles to operational risk and the cost of fraud. *Expert Systems with Applications*, 41, 2014.
- K.-M. Wang and Y.-M. Lee. Are life insurance futures a safe haven during covid-19? *Financial Innovation*, 9, 2023.
- S. Xie and C. Gan. Classification of territory risk by generalized linear and generalized linear mixed models. *Journal of Management Analytics*, 10(2), 2023.
- Y. Yang, W. Qian, and H. Zou. Insurance premium prediction via gradient tree-boosted Tweedie compound Poisson models. *Journal of Business & Economic Statistics*, 36(3):456–470, 2018.
- X. Zhong and D. Enke. Predicting the daily return direction of the stock market using hybrid machine learning algorithms. *Financial Innovation*, 5(1), 2019.
- H. Zhou, W. Qian, and Y. Yang. Tweedie gradient boosting for extremely unbalanced zero-inflated data. *Communications in Statistics-Simulation and Computation*, online:1–23, 2020.